Hindawi Publishing Corporation
Abstract and Applied Analysis
Volume 2014, Article ID 326354, 12 pages
http://dx.doi.org/10.1155/2014/326354

Research Article

A New Fractional-Order Chaotic Complex System and Its Antisynchronization

Cuimei Jiang,[1] Shutang Liu,[1] and Chao Luo[2,3]

[1] *College of Control Science and Engineering, Shandong University, Jinan 250061, China*
[2] *School of Information Science and Engineering, Shandong Normal University, Jinan 250014, China*
[3] *Shandong Provincial Key Laboratory for Novel Distributed Computer Software Technology, Jinan 250014, China*

Correspondence should be addressed to Shutang Liu; stliu@sdu.edu.cn

Received 28 March 2014; Revised 28 July 2014; Accepted 28 August 2014; Published 20 October 2014

Academic Editor: Felix Sadyrbaev

We propose a new fractional-order chaotic complex system and study its dynamical properties including symmetry, equilibria and their stability, and chaotic attractors. Chaotic behavior is verified with phase portraits, bifurcation diagrams, the histories, and the largest Lyapunov exponents. And we find that chaos exists in this system with orders less than 5 by numerical simulation. Additionally, antisynchronization of different fractional-order chaotic complex systems is considered based on the stability theory of fractional-order systems. This new system and the fractional-order complex Lorenz system can achieve antisynchronization. Corresponding numerical simulations show the effectiveness and feasibility of the scheme.

1. Introduction

Chaotic behavior and synchronization of fractional-order dynamical systems have been extensively studied over the last decade. Many fractional-order systems can behave chaotically, such as the fractional-order Chua's system [1], the fractional Rössler system [2], the fractional-order Lorenz system [3], the fractional-order Chen system [4], and the fractional-order Lü system [5]. It has been shown that some fractional-order systems have chaotic behavior with orders less than 3. Meanwhile, chaos synchronization of fractional-order systems has attracted much attention, such as the complete synchronization (CS) [6], projective synchronization (PS) [7], and lag projective synchronization [8].

However, most of the studies about fractional-order systems had been based on real variables, and complex systems are rarely involved. Complex systems provide an excellent instrument to describe a variety of physical phenomena, such as detuned laser systems, amplitudes of electromagnetic fields, and thermal convection of liquid flows [9–11]. And now complex systems have played an important role in many branches of physics, for example, superconductors, plasma physics, geophysical fluids, modulated optical waves, and electromagnetic fields [12]. There are some new kinds of synchronization for complex dynamical systems, for example, complex complete synchronization (CCS) [13], complex projective synchronization (CPS) [14], complex modified projective synchronization (CMPS) [15, 16], and so forth. These new kinds of synchronization have been widely studied for applications in secure communication [17], because complex variables (doubling the number of variables) increase the contents and security of the transmitted information. Therefore, the dynamical behavior and synchronization of the fractional-order complex nonlinear systems are worth studying. Recently, Luo and Wang proposed the fractional-order complex Lorenz system [18] and the fractional-order complex Chen system [19] and studied their dynamical properties and chaos synchronization. To our best knowledge, there are few results on fractional-order chaotic complex systems until now.

Motivated by the above discussion, the aim of this paper is to investigate the chaotic phenomena in a newly proposed fractional-order complex Lü system, which may provide potential applications in secure communication. As will be shown below, this new system displays many interesting dynamical behaviors, such as fixed points, periodic motions, and chaotic motions. Besides, when the parameters of the system are fixed, the lowest order for chaos to exist is determined. Furthermore, antisynchronization between the new system and fractional-order complex Lorenz system is studied. More generally, we investigate antisynchronization of different fractional-order chaotic complex systems and give a usual scheme.

The remainder of this paper is organized as follows. In Section 2, The fractional-order complex Lü system is presented and its dynamics is discussed by phase portraits, bifurcation diagrams, the histories, and the largest Lyapunov exponents. In Section 3, the antisynchronization of different fractional-order chaotic complex systems is studied, and the proposed new system can antisynchronize the fractional-order complex Lorenz system. A concluding remark is given in Section 4.

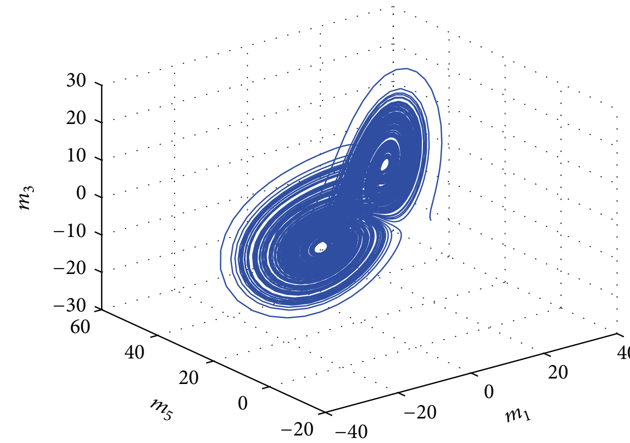

Figure 1: Chaotic attractor of complex Lü system $(a_1, a_2, a_3) = (40, 22, 5)$.

2. The Fractional-Order Complex Lü System

2.1. The Proposal of the Fractional-Order Complex Lü System. There are many definitions of fractional derivatives [20, 21], such as Riemann-Liouville, Grünwald-Letnikov, and Caputo definitions. In this paper, we use the Caputo definition which is defined as follows:

$$D_*^{\alpha} x(t) = J^{n-\alpha} x^{(n)}(t). \tag{1}$$

Here n is the first integer which is not less than α and $\alpha > 0$, $x^{(n)}$ is the n-order derivative in the usual sense, and J^{β} $(\beta > 0)$ is the β-order Riemann-Liouville integral operator with expression

$$J^{\beta}\varphi(t) = \frac{1}{\Gamma(\beta)} \int_0^t (t-\tau)^{\beta-1} \varphi(\tau)\, d\tau. \tag{2}$$

Here Γ stands for Gamma function, and the operator D_*^{α} is generally called α-order Caputo differential operator.

In 2007, the complex Lü system was proposed by Mahmoud et al. [22], which can be described as

$$\begin{aligned} \dot{x}_1 &= a_1 (x_2 - x_1), \\ \dot{x}_2 &= -x_1 x_3 + a_2 x_2, \\ \dot{x}_3 &= \frac{1}{2}(\overline{x}_1 x_2 + x_1 \overline{x}_2) - a_3 x_3, \end{aligned} \tag{3}$$

where $x = (x_1, x_2, x_3)^T$ is the vector of state variables, $x_1 = m_1 + jm_2$ and $x_2 = m_3 + jm_4$ are complex variables, and $x_3 = m_5$ is a real variable. $j = \sqrt{-1}$, $a_i > 0$ $(i = 1, 2, 3)$ is the system real parameter. When the parameters are chosen as $a_1 = 40$, $a_2 = 22$, $a_3 = 5$, the system (3) is chaotic as shown in Figure 1.

In this paper, we modify the derivative operator in (3) to be with respect to the fractional order α $(0 < \alpha \le 1)$. Thus, the fractional-order complex Lü system can be expressed by

$$\begin{aligned} D_*^{\alpha_1} x_1 &= a_1 (x_2 - x_1), \\ D_*^{\alpha_2} x_2 &= -x_1 x_3 + a_2 x_2, \\ D_*^{\alpha_3} x_3 &= \frac{1}{2}(\overline{x}_1 x_2 + x_1 \overline{x}_2) - a_3 x_3; \end{aligned} \tag{4}$$

when the derivative order $\alpha_i = 1$ $(i = 1, 2, 3)$, system (4) will be the common integer-order complex Lü system. The Caputo differential operator is a linear operator [20]; that is, $D_*^{\alpha}(ay(t) + bz(t)) = aD_*^{\alpha}(y(t)) + bD_*^{\alpha}(z(t))$, for arbitrary constants a and b. Therefore, $D_*^{\alpha_i}(x_i) = D_*^{\alpha_i}(m_{2i-1} + jm_{2i}) = D_*^{\alpha_i} m_{2i-1} + jD_*^{\alpha_i} m_{2i}$, $(i = 1, 2, 3)$.

Separating the real and imaginary parts of system (4), we can obtain the following system:

$$\begin{aligned} D_*^{\alpha_1} m_1 &= a_1 (m_3 - m_1), \\ D_*^{\alpha_1} m_2 &= a_1 (m_4 - m_2), \\ D_*^{\alpha_2} m_3 &= -m_1 m_5 + a_2 m_3, \\ D_*^{\alpha_2} m_4 &= -m_2 m_5 + a_2 m_4, \\ D_*^{\alpha_3} m_5 &= m_1 m_3 + m_2 m_4 - a_3 m_5. \end{aligned} \tag{5}$$

2.2. Numerical Algorithm for the Fractional-Order Complex Lü System. In 2002, Diethelm et al. proposed the Adams-Bashforth-Moulton predictor-corrector scheme [23], which is numerically stable and can be used to both linear and nonlinear fractional differential equations.

According to this algorithm, system (5) for initial condition $(m_{10}, m_{20}, m_{30}, m_{40}, m_{50})$ can be discretized as

$$\begin{aligned}
m_{1,n+1} &= m_{10} + \frac{h^{\alpha_1}}{\Gamma(\alpha_1+2)} \\
&\quad \times \left[a_1\left(m^p_{3,n+1} - m^p_{1,n+1}\right) \right. \\
&\qquad \left. + \sum_{j=0}^{n} \gamma_{1,j,n+1} a_1\left(m_{3j} - m_{1j}\right) \right], \\
m_{2,n+1} &= m_{20} + \frac{h^{\alpha_1}}{\Gamma(\alpha_1+2)} \\
&\quad \times \left[a_1\left(m^p_{4,n+1} - m^p_{2,n+1}\right) \right. \\
&\qquad \left. + \sum_{j=0}^{n} \gamma_{1,j,n+1} a_1\left(m_{4j} - m_{2j}\right) \right], \\
m_{3,n+1} &= m_{30} + \frac{h^{\alpha_2}}{\Gamma(\alpha_2+2)} \\
&\quad \times \left[a_2 m^p_{3,n+1} - m^p_{1,n+1} m^p_{5,n+1} \right. \\
&\qquad \left. + \sum_{j=0}^{n} \gamma_{2,j,n+1} \left(a_2 m_{3j} - m_{1j} m_{5j}\right) \right], \\
m_{4,n+1} &= m_{40} + \frac{h^{\alpha_2}}{\Gamma(\alpha_2+2)} \\
&\quad \times \left[a_2 m^p_{4,n+1} - m^p_{2,n+1} m^p_{5,n+1} \right. \\
&\qquad \left. + \sum_{j=0}^{n} \gamma_{2,j,n+1} \left(a_2 m_{4j} - m_{2j} m_{5j}\right) \right], \\
m_{5,n+1} &= m_{50} + \frac{h^{\alpha_3}}{\Gamma(\alpha_3+2)} \\
&\quad \times \left[m^p_{1,n+1} m^p_{3,n+1} + m^p_{2,n+1} m^p_{4,n+1} - a_3 m^p_{5,n+1} \right. \\
&\qquad \left. + \sum_{j=0}^{n} \gamma_{3,j,n+1} \left(m_{1j} m_{3j} + m_{2j} m_{4j} - a_3 m_{5j}\right) \right],
\end{aligned} \tag{6}$$

where

$$\begin{aligned}
m^p_{1,n+1} &= m_{10} + \frac{1}{\Gamma(\alpha_1)} \sum_{j=0}^{n} \omega_{1,j,n+1} a_1\left(m_{3j} - m_{1j}\right), \\
m^p_{2,n+1} &= m_{20} + \frac{1}{\Gamma(\alpha_1)} \sum_{j=0}^{n} \omega_{1,j,n+1} a_2\left(m_{4j} - m_{2j}\right), \\
m^p_{3,n+1} &= m_{30} + \frac{1}{\Gamma(\alpha_2)} \sum_{j=0}^{n} \omega_{2,j,n+1} \left(a_2 m_{3j} - m_{1j} m_{5j}\right), \\
m^p_{4,n+1} &= m_{40} + \frac{1}{\Gamma(\alpha_2)} \sum_{j=0}^{n} \omega_{2,j,n+1} \left(a_2 m_{4j} - m_{2j} m_{5j}\right), \\
m^p_{5,n+1} &= m_{50} \\
&\quad + \frac{1}{\Gamma(\alpha_3)} \sum_{j=0}^{n} \omega_{3,j,n+1} \left(m_{1j} m_{3j} + m_{2j} m_{4j} - a_3 m_{5j}\right), \\
&\gamma_{i,j,n+1} \\
&= \begin{cases} n^{\alpha_i+1} - (n-\alpha_i)(n+1)^{\alpha_i}, & j = 0, \\ (n-j+2)^{\alpha_i+1} + (n-j)^{\alpha_i+1} & \\ \quad -2(n-j+1)^{\alpha_i+1}, & 1 \le j \le n, \\ 1, & j = n+1, \end{cases} \\
\omega_{i,j,n+1} &= \frac{h^{\alpha_i}}{\alpha_i}\left((n+1-j)^{\alpha_i} - (n-j)^{\alpha_i}\right).
\end{aligned} \tag{7}$$

2.3. Dynamics of the Fractional-Order Complex Lü System

2.3.1. Symmetry and Invariance. Note that the symmetry of system (5) is symmetric about m_5-axis, which means it is invariant for the coordinate transformation of $(m_1, m_2, m_3, m_4, m_5) \to (-m_1, -m_2, -m_3, -m_4, m_5)$.

2.3.2. Equilibria and Stability. The equilibria of system (5) can be calculated by solving the equations $D_*^{\alpha_j} m_i = 0$ ($j = 1, 2, 3$; $i = 1, 2, \ldots, 5$), and this system has an isolated equilibria $E_0 = (0, 0, 0, 0, 0)$ and nontrivial equilibria $E_\theta = (r\cos\theta, r\sin\theta, r\cos\theta, r\sin\theta, a_2)$, where $r = \sqrt{a_2 a_3}$, $\theta \in [0, 2\pi]$.

As to the equilibrium E_0, it is stable when $a_2 < 0$ and unstable when $a_2 > 0$. For E_θ, the characteristic polynomial of Jacobian matrix is $\lambda(\lambda + a_1 - a_2)(\lambda^3 + (a_1 + a_3 - a_2)\lambda^2 + a_1 a_3 \lambda + 2a_1 a_2 a_3) = 0$ when $a_2 > 0$. According to the fractional-order Routh-Hurwitz conditions [24], when $(a_1 + a_3 - a_2) \cdot (a_1 a_3) > 2a_1 a_2 a_3$, E_θ will be stable.

2.3.3. Chaotic Behavior and Attractors. Using the above discretization scheme (6), we find that chaotic behaviors exist in the fractional-order complex Lü system. In the numerical simulations, the system parameters are chosen as $(a_1, a_2, a_3) = (42, 22, 5)$, and an initial value is $(x_1, x_2, x_3)^T = (1 + 2j, 3 + 4j, 5)^T$. When varying the fractional derivative order α_i ($i = 1, 2, 3$), system (5) will display diverse motions. The existence of chaos is demonstrated with the time histories, phase diagrams, bifurcation diagrams, and the largest Lyapunov exponents. It is well known that there are many

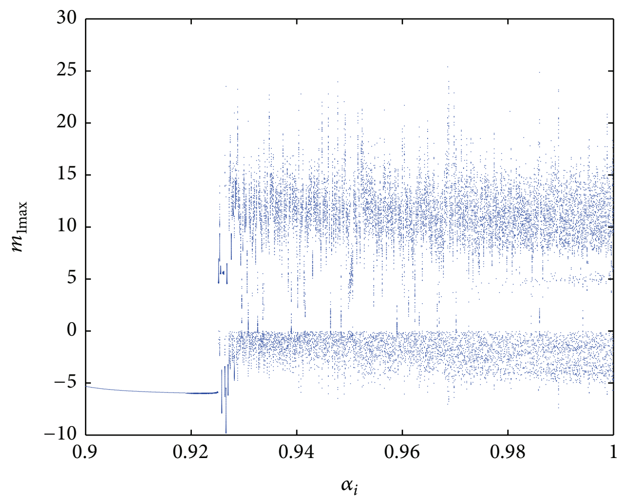

Figure 2: Bifurcation diagram of system (5) with $\alpha_1 = \alpha_2 = \alpha_3 = \alpha \in [0.9, 1]$.

effective algorithms for the calculation of the Lyapunov exponents [25–27]. In this paper, the largest Lyapunov exponents are calculated by Wolf algorithm [25].

(1) Commensurate Order $\alpha_1 = \alpha_2 = \alpha_3 = \alpha$. The bifurcation diagram is calculated numerically against $\alpha \in [0.9, 1]$, while the incremental value of α is 0.0002. From the bifurcation diagram shown in Figure 2, it is found that chaotic range is $\alpha \in [0.928, 1]$. To identify the route to chaos, the time history of m_5 is shown in Figures 3(a)–3(d). It is clearly shown that the state variables are stable at the fixed point at $\alpha = 0.922$, which can be seen in Figure 3(a). When α increases, intermittent dynamical behavior is observed in Figures 3(b)-3(c). As α is further increased, the motion become chaotic as shown for $\alpha = 0.928$, where the largest Lyapunov exponent is $\lambda = 0.0154$. In Figures 4(a)-4(b), phase portraits are shown at $\alpha = 0.927$ and 0.928, respectively. Numerical evidence displays that the lowest order to yield chaos is 4.64, where $\alpha = 0.928$.

(2) $\alpha_2 = \alpha_3 = 1$, and Let α_1 Vary. The bifurcation diagram is calculated numerically against $\alpha_1 \in [0.78, 1]$, while the incremental value of α_1 is 0.0002. Figure 5 shows that chaotic motions exist in the range $\alpha_1 \in [0.812, 1]$. To identify the route to chaos, the time history of m_5 is shown in Figures 6(a)–6(d). At $\alpha_1 = 0.807$, the state variables are stable at the fixed point as depicted in Figure 6(a). When α_1 increases, intermittent dynamical behavior is observed in Figures 6(b)-6(c). As α_1 is further increased, the motion become chaotic as shown for $\alpha_1 = 0.812$, where the largest Lyapunov exponent is $\lambda = 0.0899$. In this case, the lowest order for system (5) to be chaotic is 4.624, where $\alpha_1 = 0.812$.

(3) $\alpha_1 = \alpha_3 = 1$, and Let α_2 Vary. The bifurcation diagram is calculated numerically against $\alpha_2 \in [0.75, 1]$, while the incremental value of α is 0.0005. Figure 7(a) shows that the chaotic zone covers most of the range of $\alpha_2 \in [0.805, 1]$. To observe the dynamical behavior of system, the region of $\alpha_2 \in [0.75, 0.85]$ is expanded in step size of 0.0002 as shown in Figure 7(b). The period-doubling bifurcations can be seen in Figure 7(b). Phase diagrams shown in Figures 8(a)–8(d) exhibit period-1, period-2, period-4, and chaotic behaviors. Thus, Figure 8 identifies a period doubling route to chaos. In this case, the lowest order for system (5) to be chaotic is 4.61, where $\alpha_2 = 0.805$ and the largest Lyapunov exponent is $\lambda = 0.0461$.

(4) $\alpha_1 = \alpha_2 = 1$, and Let α_3 Vary. The system is calculated numerically against $\alpha_3 \in [0.8, 1]$ with the step size of 0.001. Figures 9(a)–9(d) displays the phase portraits at $\alpha_3 = 0.830, 0.831, 0.90$ and 0.950, respectively. Results show that chaos exists in the range $\alpha_3 \in [0.831, 1]$. To identify the route to chaos, the time history of m_5 is shown in Figures 10(a)–10(d). At $\alpha_1 = 0.820$, the state variables are stable at the fixed point as depicted in Figure 10(a). When α increases, intermittent dynamical behavior is observed in Figures 10(b)-10(c). As α is further increased, the motion become chaotic as shown for $\alpha = 0.831$, where the largest Lyapunov exponent is $\lambda = 0.0516$. Numerical evidence displays that the lowest order for system (5) to be chaotic is 4.831, where $\alpha_3 = 0.831$.

3. Antisynchronization between Different Fractional-Order Complex Systems

In this section, we give a general method to achieve antisynchronization of different fractional-order complex systems firstly. Consequently, antisynchronization between fractional-order complex Lü and Lorenz system can be achieved. Without loss of generality, we assume that the derivative order is α $(\alpha < 1)$ in both master system and slave system.

3.1. A General Method for Antisynchronization of Fractional-Order Complex Systems. Consider the following fractional-order complex system:

$$D_*^\alpha x = Ax + f(x), \tag{8}$$

where $x = (x_1, x_2, \ldots, x_n)^T$ is the state complex vector, $x = x^r + jx^i$, and define $x_1 = m_1 + jm_2$, $x_2 = m_3 + jm_4, \ldots, x_n = m_{2n-1} + jm_{2n}$. $f = (f_1, f_2, \ldots, f_n)^T$ is a vector of nonlinear complex functions and $A \in R^{n\times n}$ is the matrix of system parameters. Superscripts r and i stand for the real and imaginary parts of the state complex vector. System (8) is considered as the master system and the slave system is given by

$$D_*^\alpha y = By + g(y) + u, \tag{9}$$

where $y = (y_1, y_2, \ldots, y_n)^T$ is the state complex vector, $y = y^r + jy^i$, and define $y_1 = s_1 + js_2$, $y_2 = s_3 + js_4, \ldots, y_n = s_{2n-1} + js_{2n}$. $u = u^r + ju^i$ is designed controller, where $u^r = (u_1, u_3, \ldots, u_{2n-1})^T$, $u^i = (u_2, u_4, \ldots, u_{2n})^T$.

Remark 1. Some fractional-order chaotic complex systems can be described by (8), such as the fractional-order complex Lorenz, Lü, and Chen systems.

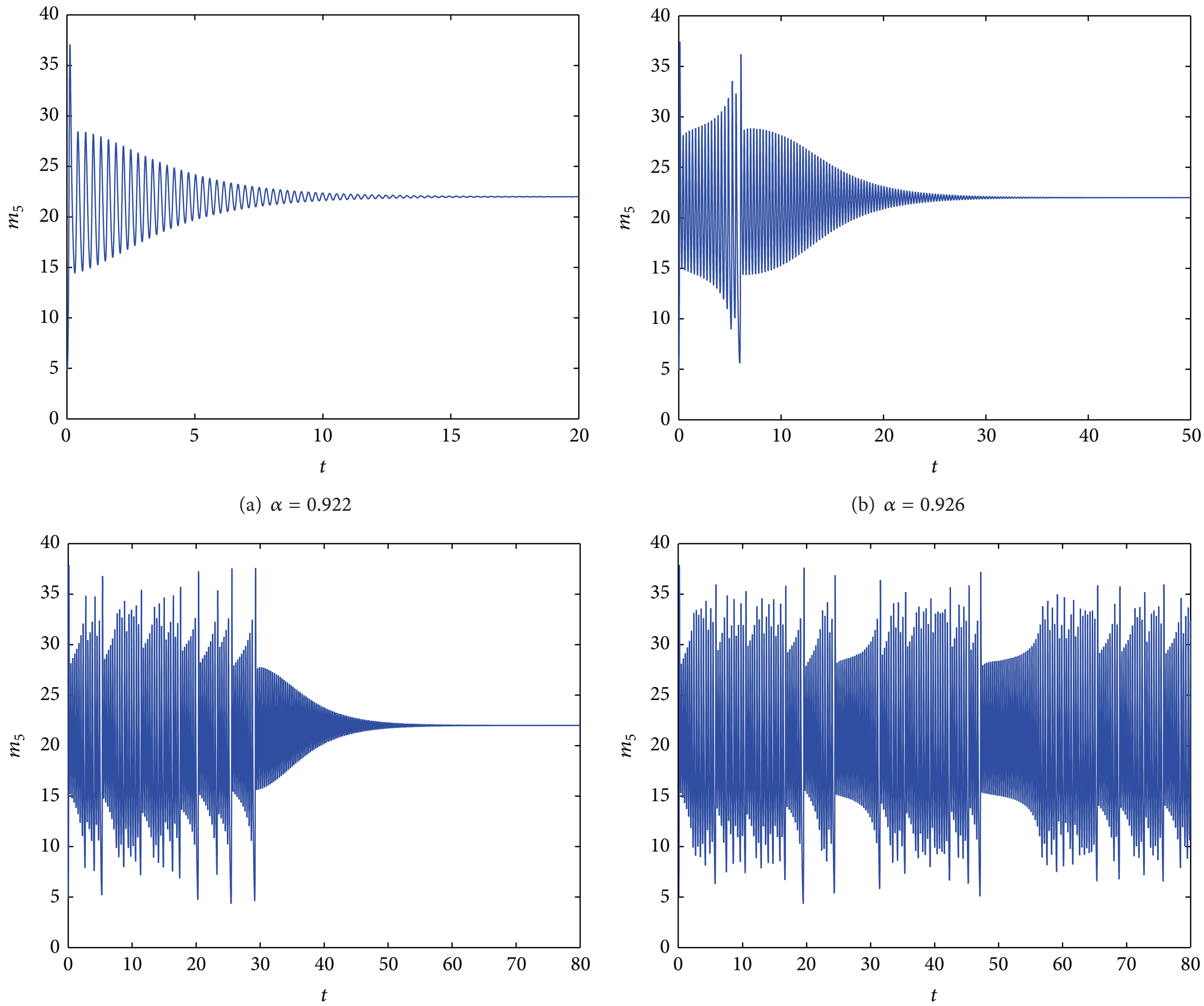

(a) $\alpha = 0.922$

(b) $\alpha = 0.926$

(c) $\alpha = 0.927$

(d) $\alpha = 0.928$

FIGURE 3: Time histories showing the rout to chaos via intermittency for system (5) at $\alpha_1 = \alpha_2 = \alpha_3 = \alpha$.

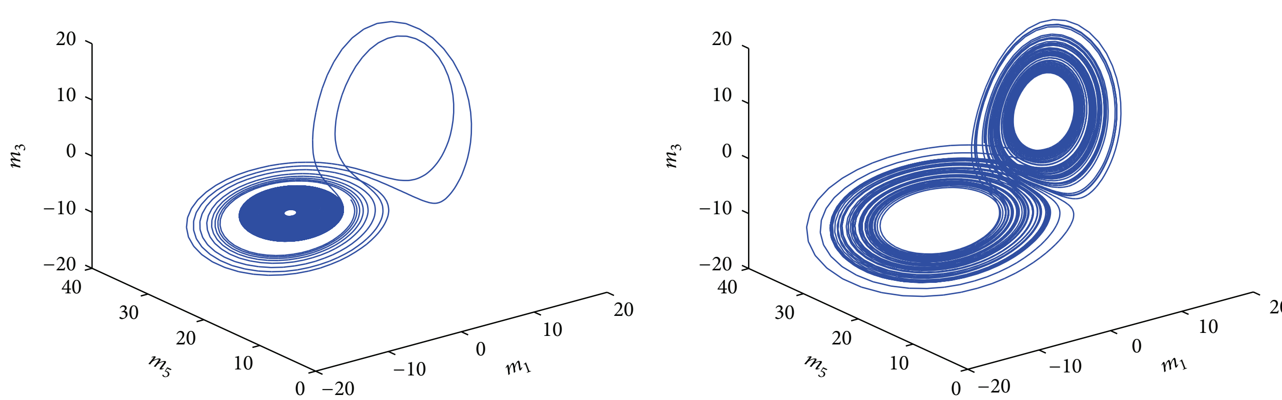

(a) $\alpha = 0.927$

(b) $\alpha = 0.928$

FIGURE 4: Phase portraits of system (5) at $\alpha_1 = \alpha_2 = \alpha_3 = \alpha$.

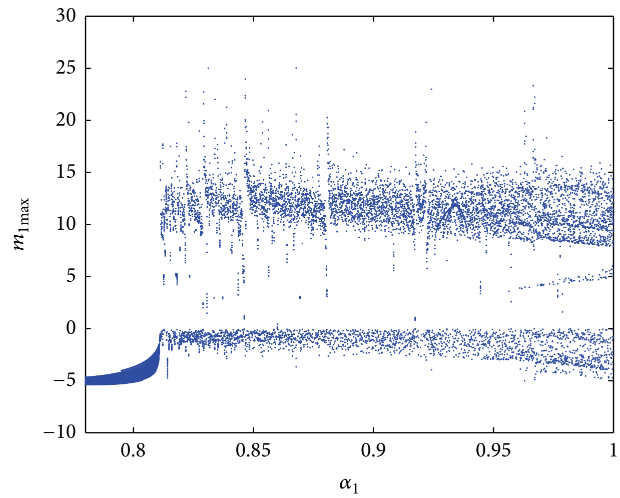

Figure 5: Bifurcation diagram of system (5) with $\alpha_1 \in [0.78, 1]$.

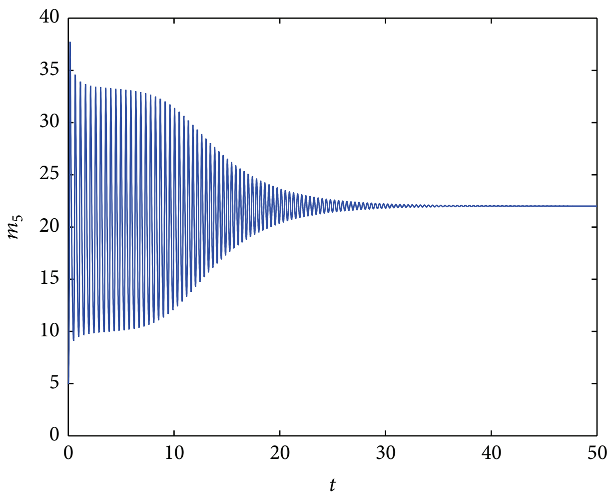

(a) $\alpha_1 = 0.807$

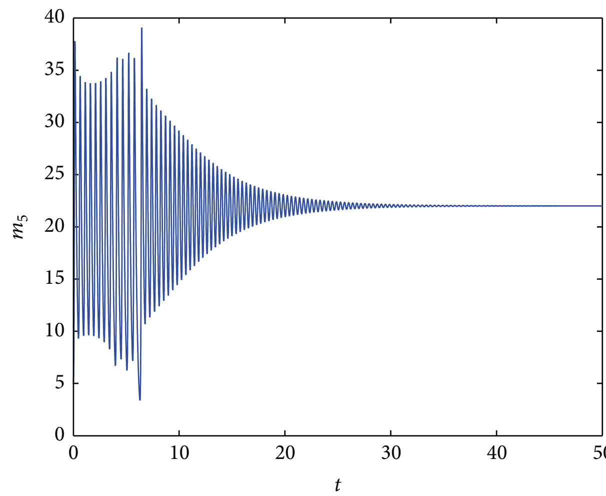

(b) $\alpha_1 = 0.810$

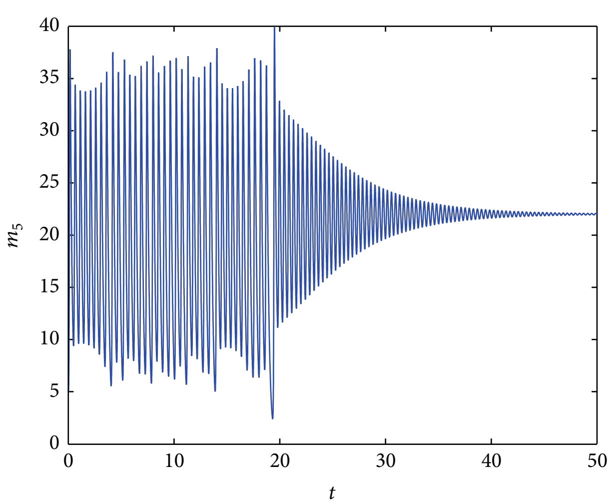

(c) $\alpha_1 = 0.811$

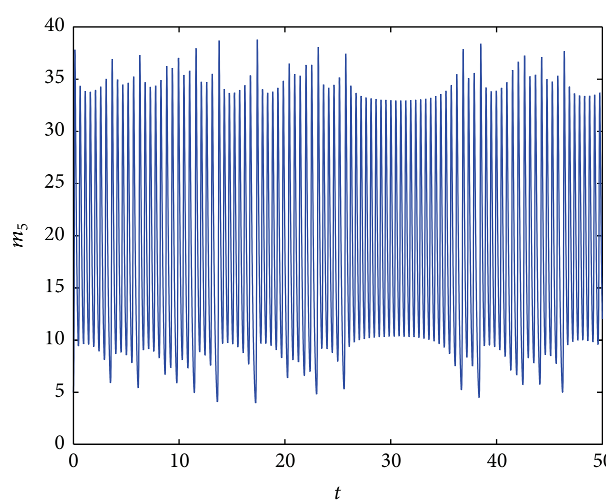

(d) $\alpha_1 = 0.812$

Figure 6: Time histories showing the rout to chaos via intermittency for system (5) at $\alpha_2 = \alpha_3 = 1$ with α_1 varying.

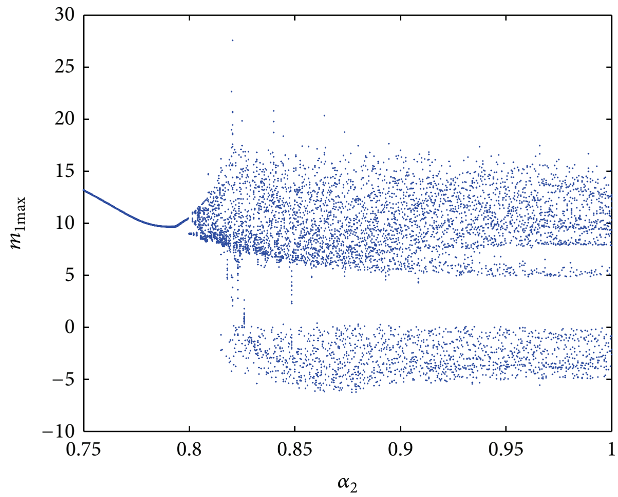

(a) $\alpha_2 \in (0.75, 1)$

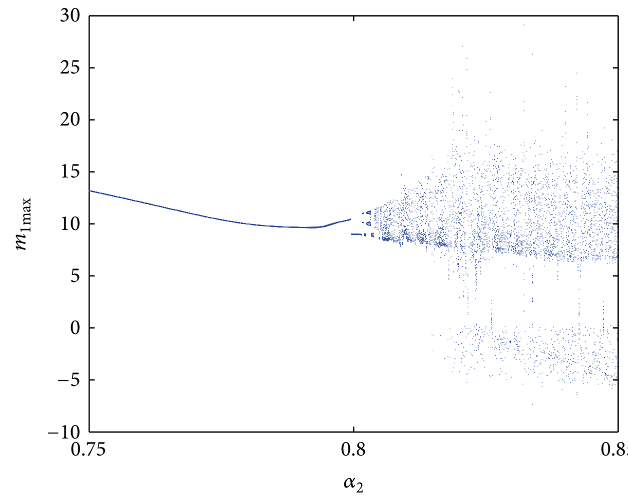

(b) $\alpha_2 \in (0.75, 0.85)$

FIGURE 7: Bifurcation diagram of system (5) at $\alpha_1 = \alpha_3 = 1$ with α_2 varying.

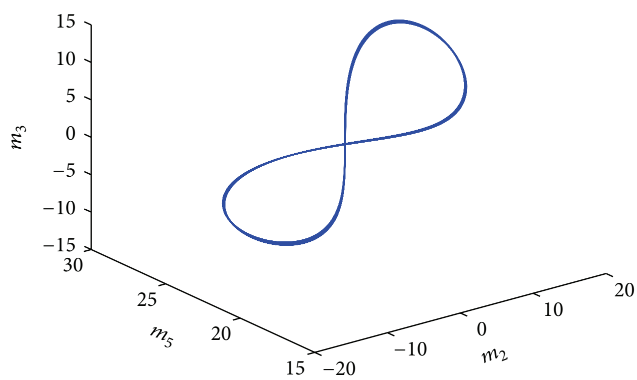

(a) $\alpha_2 = 0.801$

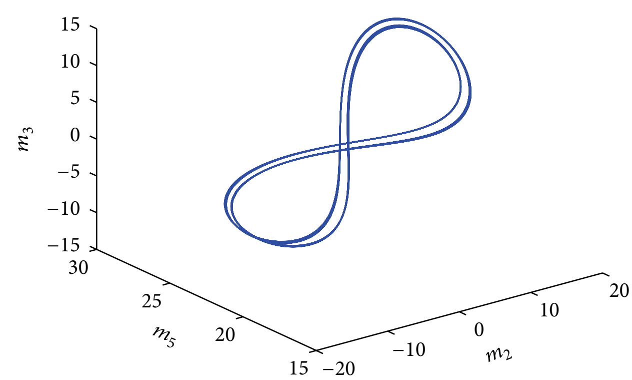

(b) $\alpha_2 = 0.802$

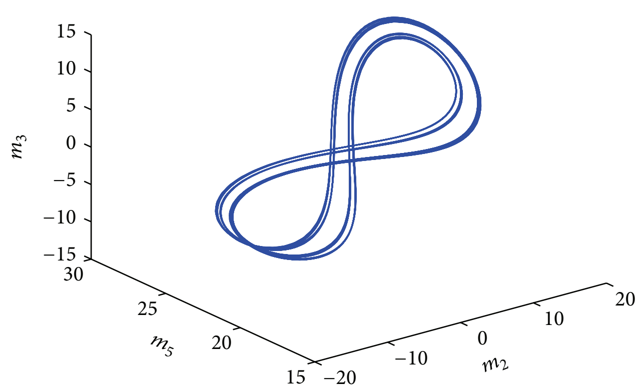

(c) $\alpha_2 = 0.804$

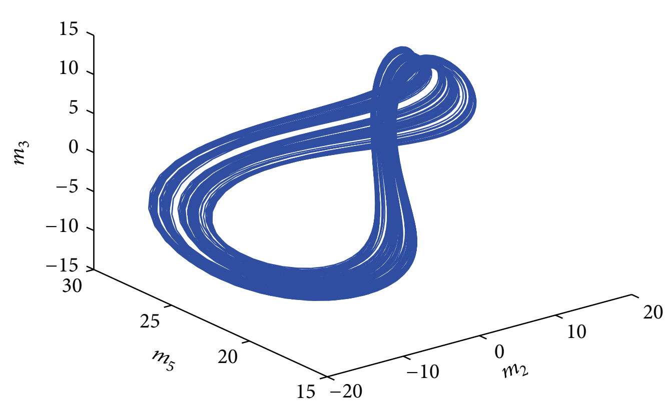

(d) $\alpha_2 = 0.805$

FIGURE 8: Phase portraits of system (6) at $\alpha_1 = \alpha_3 = 1$ with α_2 varying.

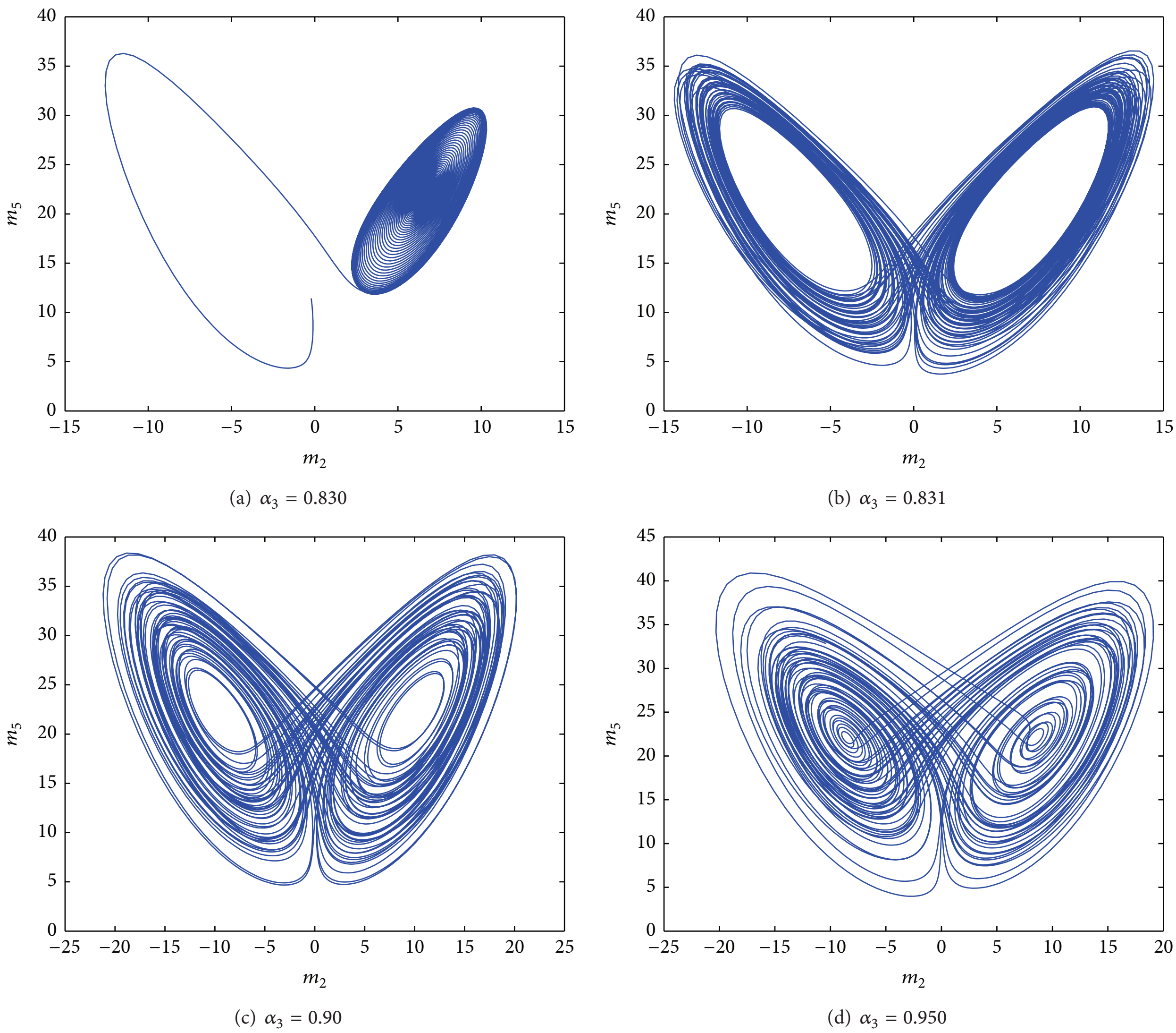

(a) $\alpha_3 = 0.830$ (b) $\alpha_3 = 0.831$ (c) $\alpha_3 = 0.90$ (d) $\alpha_3 = 0.950$

Figure 9: Phase portraits of system (5) at $\alpha_1 = \alpha_2 = 1$ with α_3 varying.

Now we give the stability results for linear fractional-order systems.

Lemma 2 (see [28]). *Autonomous linear system of the fractional-order* $D_*^{\alpha}x = Ax$, *with* $x(0) = x_0$ *is asymptotically stable if and only if* $|\arg(\lambda_i(A))| > \alpha\pi/2$, $(i = 1, 2, 3 \ldots)$. *In this case, the component of the state decay towards* 0 *like* $t^{-\alpha}$. *Also, this system is stable if and only if either it is asymptotically stable or those critical eigenvalues which satisfy* $|\arg(\lambda_i(A))| = \alpha\pi/2$ *have geometric multiplicity one, where* $\arg(\lambda_i(A))$ *denotes the argument of the eigenvalue* λ_i *of* A.

Theorem 3. *Antisynchronization between* (8) *and* (9) *will be achieved, if the controller is designed as follows:*

$$u(t) = u^r + ju^i = -f(x) - g(y) + (B - A)x - Ke. \quad (10)$$

The real and imaginary parts of (10) *are*

$$\begin{aligned} u^r &= -f^r(x) - g^r(y) + (B - A)x^r - Ke^r, \\ u^i &= -f^i(x) - g^i(y) + (B - A)x^i - Ke^i; \end{aligned} \quad (11)$$

here K *is the control gain matrix, which satisfies* $|\arg(\lambda_i(B - K))| > \alpha\pi/2$ *for all the eigenvalues of* $B - K$.

Proof. From the definition of antisynchronization, we obtain the error vector between (8) and (9) as follows:

$$e(t) = y(t) + x(t), \quad (12)$$

The derivative of the error vector (12) can be expressed as

$$\begin{aligned} D_*^{\alpha}e(t) &= D_*^{\alpha}y(t) + D_*^{\alpha}x(t) \\ &= By + g(y) + u + Ax + f(x), \end{aligned} \quad (13)$$

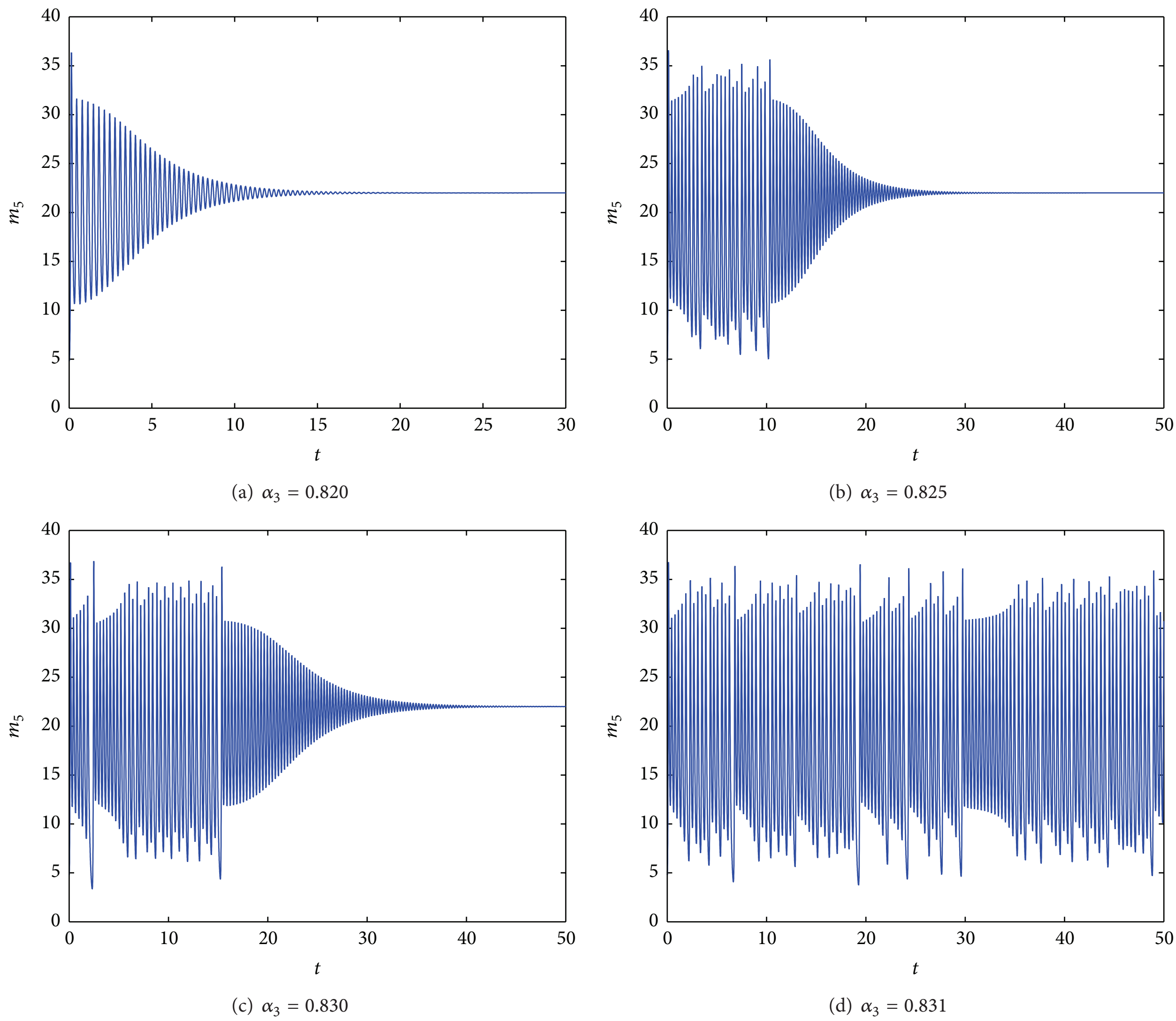

FIGURE 10: Time histories showing the rout to chaos via intermittency for system (5) at $\alpha_1 = \alpha_2 = 1$ with α_3 varying.

Substituting (10) into (13), the error dynamical system (13) can be written as

$$D_*^{\alpha} e(t) = (B - K) e(t). \quad (14)$$

Since $|\arg(\lambda_i(B-K))| > \alpha\pi/2$, according to Lemma 2, the error vector $e(t)$ asymptotically converges to zero as $t \to \infty$. So antisynchronization between different fractional-order complex systems is achieved by using the controller (10). This completes the proof. □

Remark 4. If $A = B$ and $f(\cdot) = g(\cdot)$, systems (8) and (9) become identical. Therefore, our scheme is also applicable to achieve antisynchronization of two identical fractional-order chaotic complex systems.

3.2. Antisynchronization between Fractional-Order Complex Lü and Lorenz System. In this section, the antisynchronization behavior between the fractional-order complex Lü and Lorenz systems is made. It is assumed that the fractional-order complex Lü system drives the fractional-order complex Lorenz system [18]. Thus the master system is described by

$$\begin{aligned} D_*^{\alpha_1} x_{1m} &= a_1 (x_{2m} - x_{1m}), \\ D_*^{\alpha_2} x_{2m} &= -x_{1m}x_{3m} + a_2 x_{2m}, \\ D_*^{\alpha_3} x_{3m} &= \frac{1}{2}(\overline{x}_{1m}x_{2m} + x_{1m}\overline{x}_{2m}) - a_3 x_{3m}, \end{aligned} \quad (15)$$

where

$$A = \begin{pmatrix} -a_1 & a_1 & 0 \\ 0 & a_2 & 0 \\ 0 & 0 & -a_3 \end{pmatrix},$$
$$f(x) = \begin{pmatrix} 0 \\ -x_{1m}x_{3m} \\ \frac{1}{2}(\overline{x}_{1m}x_{2m} + x_{1m}\overline{x}_{2m}) \end{pmatrix}. \quad (16)$$

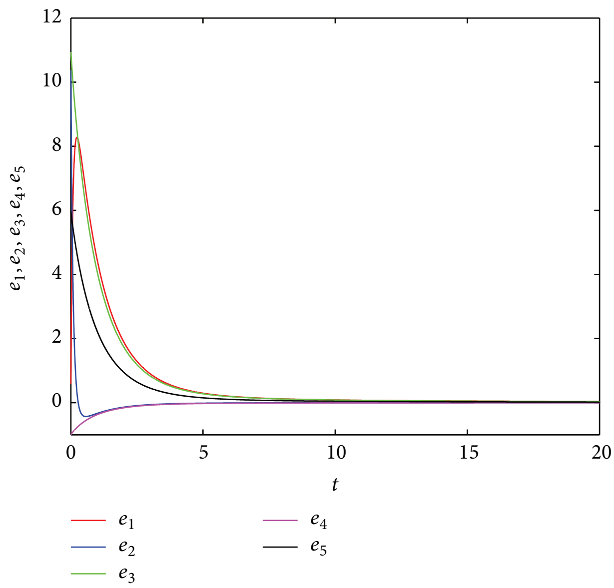

FIGURE 11: The time evolution of the synchronization errors between systems (15) and (17) (time/s).

The slave system is

$$
\begin{aligned}
D_*^{\alpha_1} x_{1s} &= b_1 \left(x_{2s} - x_{1s}\right) + u_1 + j u_2, \\
D_*^{\alpha_2} x_{2s} &= b_2 x_{1s} - x_{2s} - x_{1s} x_{3s} + u_3 + j u_4, \\
D_*^{\alpha_3} x_{3s} &= \frac{1}{2} \left(\overline{x}_{1s} x_{2s} + x_{1s} \overline{x}_{2s}\right) - b_3 x_{3s} + u_5,
\end{aligned}
\tag{17}
$$

where

$$
\begin{aligned}
B &= \begin{pmatrix} -b_1 & b_1 & 0 \\ b_2 & -1 & 0 \\ 0 & 0 & -b_3 \end{pmatrix}, \\
g(y) &= \begin{pmatrix} 0 \\ -x_{1s} x_{3s} \\ \frac{1}{2} \left(\overline{x}_{1s} x_{2s} + x_{1s} \overline{x}_{2s}\right) \end{pmatrix}.
\end{aligned}
\tag{18}
$$

In the numerical simulations, the initial values of the master and slave systems are $(x_{1m}, x_{2m}, x_{3m})^T = (1 + 2j, 3 + 4j, 5)^T$ and $(x_{1s}, x_{2s}, x_{3s})^T = (-1 + 9j, 8 - 5j, 1)^T$, respectively. Choose the parameters of the master and slave system as $(a_1, a_2, a_3) = (42, 22, 5)$, $(b_1, b_2, b_3) = (10, 180, 1)$, $\alpha_1 = \alpha_2 = \alpha_3 = 0.95$. In order to satisfy $|\arg(\lambda_i(B - K))| > \alpha\pi/2$, we choose the gain control matrix K as follows:

$$
K = \begin{pmatrix} 0 & 0 & 0 \\ 180 & 0 & 0 \\ 0 & 0 & 0 \end{pmatrix}.
\tag{19}
$$

According to Theorem 3, the controller is designed as

$$
\begin{aligned}
u = &- \begin{pmatrix} 0 \\ -x_{1m} x_{3m} \\ \frac{1}{2} \left(\overline{x}_{1m} x_{2m} + x_{1m} \overline{x}_{2m}\right) \end{pmatrix} \\
&- \begin{pmatrix} 0 \\ -x_{1s} x_{3s} \\ \frac{1}{2} \left(\overline{x}_{1s} x_{2s} + x_{1s} \overline{x}_{2s}\right) \end{pmatrix} \\
&+ (B - A) \begin{pmatrix} x_{1m} \\ x_{2m} \\ x_{3m} \end{pmatrix} - K \begin{pmatrix} x_{1s} + x_{1m} \\ x_{2s} + x_{2m} \\ x_{3s} + x_{3m} \end{pmatrix} \\
= &\begin{pmatrix} \left(b_1 - a_1\right) \left(x_{2m} - x_{1m}\right) \\ x_{1m} x_{3m} + x_{1s} x_{3s} + b_2 x_{1m} - \left(a_2 + 1\right) x_{2m} - 180 \left(x_{1s} + x_{1m}\right) \\ -\frac{1}{2} \left(\overline{x}_{1m} x_{2m} + x_{1m} \overline{x}_{2m}\right) - \frac{1}{2} \left(\overline{x}_{1s} x_{2s} + x_{1s} \overline{x}_{2s}\right) + \left(a_3 - b_3\right) x_{3m} \end{pmatrix}.
\end{aligned}
\tag{20}
$$

The errors of antisynchronization converge asymptotically to zero in a quite short period as depicted in Figure 11. Figure 12 shows state variables of drive system and response system, in which the state complex variables are demonstrated by real and imaginary part, respectively. The above results verify that antisynchronization between fractional-order complex Lü system and Lorenz system has been achieved.

4. Conclusions

In this paper, a new fractional-order chaotic complex system is proposed. By means of phase portraits, bifurcation diagrams, the histories, and the largest Lyapunov exponents, we investigate chaotic behavior of this new system. Our results show that the new system displays many interesting dynamical behaviors, such as fixed points, periodic motions, and chaotic motions. Two typical routes to chaos—period doubling and intermittency—are found in this system. Besides, when the parameters of the system are fixed, the lowest order for chaos to exist is determined. Moreover, antisynchronization of different fractional-order chaotic complex systems has been studied. Meanwhile, the new system and the fractional-order complex Lorenz system can achieve antisynchronization.

Conflict of Interests

The authors declare that there is no conflict of interests regarding the publication of this paper.

Acknowledgments

The research is supported by the National Nature Science Foundation of China (nos. 61273088 and 10971120) and the Nature Science Foundation of Shandong province (no. ZR2010FM010). The authors would like to thank the editors and anonymous referees for their constructive comments and suggestions.

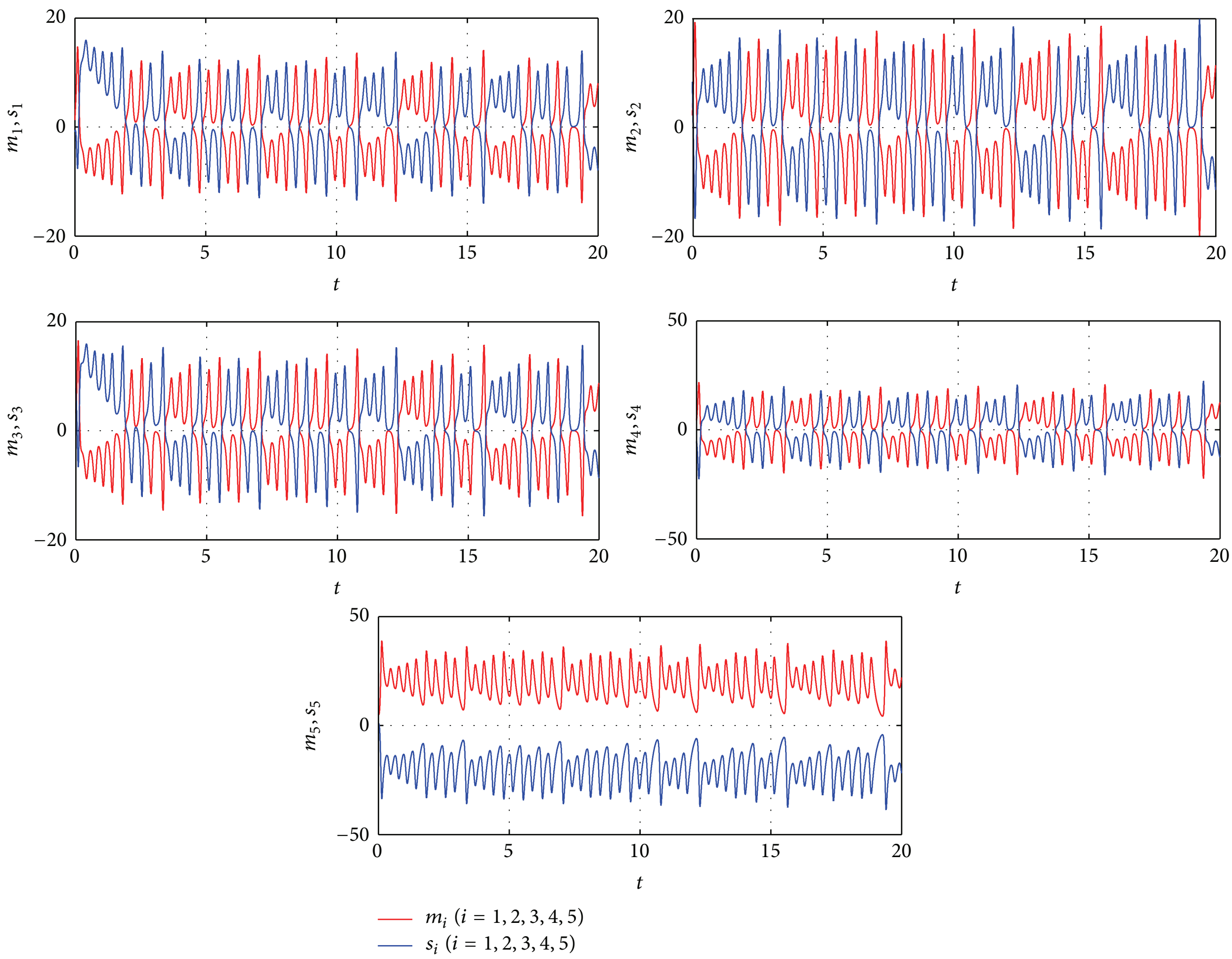

Figure 12: State variables of master system (15) and slave (17) (time/s).

References

[1] T. T. Hartley, C. F. Lorenzo, and H. K. Qammer, "Chaos in a fractional order Chua's system," *IEEE Transactions on Circuits and Systems I: Fundamental Theory and Applications*, vol. 42, no. 8, pp. 485–490, 1995.

[2] C. Li and G. Chen, "Chaos and hyperchaos in the fractional-order Rössler equations," *Physica A: Statistical Mechanics and its Applications*, vol. 341, no. 1–4, pp. 55–61, 2004.

[3] I. Grigorenko and E. Grigorenko, "Chaotic dynamics of the fractional Lorenz system," *Physical Review Letters*, vol. 91, no. 3, Article ID 034101, 2003.

[4] C. Li and G. Chen, "Chaos in the fractional order Chen system and its control," *Chaos, Solitons and Fractals*, vol. 22, no. 3, pp. 549–554, 2004.

[5] J. G. Lu, "Chaotic dynamics of the fractional-order Lü system and its synchronization," *Physics Letters A*, vol. 354, no. 4, pp. 305–311, 2006.

[6] L. Pan, W. Zhou, J. Fang, and D. Li, "Synchronization and anti-synchronization of new uncertain fractional-order modified unified chaotic systems via novel active pinning control," *Communications in Nonlinear Science and Numerical Simulation*, vol. 15, no. 12, pp. 3754–3762, 2010.

[7] G. Si, Z. Sun, Y. Zhang, and W. Chen, "Projective synchronization of different fractional-order chaotic systems with non-identical orders," *Nonlinear Analysis: Real World Applications*, vol. 13, no. 4, pp. 1761–1771, 2012.

[8] L. Chen, Y. Chai, and R. Wu, "Lag projective synchronization in fractional-order chaotic (hyperchaotic) systems," *Physics Letters A: General, Atomic and Solid State Physics*, vol. 375, no. 21, pp. 2099–2110, 2011.

[9] E. Roldán, G. J. de Valcárcel, R. Vilaseca, and P. Mandel, "Single-mode-laser phase dynamics," *Physical Review A*, vol. 48, no. 1, pp. 591–598, 1993.

[10] C.-Z. Ning and H. Haken, "Detuned lasers and the complex Lorenz equations: subcritical and supercritical Hopf bifurcations," *Physical Review A*, vol. 41, no. 7, pp. 3826–3837, 1990.

[11] V. Y. Toronov and V. L. Derbov, "Boundedness of attractors in the complex Lorenz model," *Physical Review E*, vol. 55, no. 3, pp. 3689–3692, 1997.

[12] G. M. Mahmoud and T. Bountis, "The dynamics of systems of complex nonlinear oscillators: a review," *International Journal of Bifurcation and Chaos in Applied Sciences and Engineering*, vol. 14, no. 11, pp. 3821–3846, 2004.

[13] E. E. Mahmoud, "Complex complete synchronization of two nonidentical hyperchaotic complex nonlinear systems," *Mathematical Methods in the Applied Sciences*, vol. 37, no. 3, pp. 321–328, 2014.

[14] Z. Wu, J. Duan, and X. Fu, "Complex projective synchronization in coupled chaotic complex dynamical systems," *Nonlinear Dynamics*, vol. 69, no. 3, pp. 771–779, 2012.

[15] F. Zhang and S. Liu, "Full state hybrid projective synchronization and parameters identification for uncertain chaotic (hyperchaotic) complex systems," *Journal of Computational and Nonlinear Dynamics*, vol. 9, no. 2, Article ID 021009, 2014.

[16] G. M. Mahmoud and E. E. Mahmoud, "Complex modified projective synchronization of two chaotic complex nonlinear systems," *Nonlinear Dynamics*, vol. 73, no. 4, pp. 2231–2240, 2013.

[17] S. Liu and F. Zhang, "Complex function projective synchronization of complex chaotic system and its applications in secure communication," *Nonlinear Dynamics*, vol. 76, no. 2, pp. 1087–1097, 2014.

[18] C. Luo and X. Wang, "Chaos in the fractional-order complex Lorenz system and its synchronization," *Nonlinear Dynamics*, vol. 71, no. 1-2, pp. 241–257, 2013.

[19] C. Luo and X. Wang, "Chaos generated from the fractional-order complex Chen system and its application to digital secure communication," *International Journal of Modern Physics C*, vol. 24, Article ID 1350025, 23 pages, 2013.

[20] K. B. Oldham and J. Spanier, *The Fractional Calculus*, Academic Press, San Diego, Calif, USA, 1974.

[21] I. Podlubny, *Fractional Differential Equations*, Academic Press, New York, NY, USA, 1999.

[22] G. M. Mahmoud, T. Bountis, and E. E. Mahmoud, "Active control and global synchronization of the complex Chen and Lü systems," *International Journal of Bifurcation and Chaos*, vol. 17, no. 12, pp. 4295–4308, 2007.

[23] K. Diethelm, N. J. Ford, and A. D. Freed, "A predictor-corrector approach for the numerical solution of fractional differential equations," *Nonlinear Dynamics*, vol. 29, no. 1–4, pp. 3–22, 2002.

[24] X. Wang, Y. He, and M. Wang, "Chaos control of a fractional order modified coupled dynamos system," *Nonlinear Analysis: Theory, Methods &; Applications*, vol. 71, no. 12, pp. 6126–6134, 2009.

[25] A. Wolf, J. B. Swift, H. L. Swinney, and J. A. Vastano, "Determining Lyapunov exponents from a time series," *Physica D: Nonlinear Phenomena*, vol. 16, no. 3, pp. 285–317, 1985.

[26] P. M. Pardalos and V. A. Yatsenko, "Optimization approach to the estimation and control of Lyapunov exponents," *Journal of Optimization Theory and Its Applications*, vol. 128, no. 1, pp. 29–48, 2006.

[27] S. P. Nair, D.-S. Shiau, J. C. Principe et al., "An investigation of EEG dynamics in an animal model of temporal lobe epilepsy using the maximum Lyapunov exponent," *Experimental Neurology*, vol. 216, no. 1, pp. 115–121, 2009.

[28] D. Matignon, "Stability results for fractional differential equations with applications to control processing," in *Proceedings of the International IMACS IEEE-SMC Multiconference on Computational Engineering in Systems Applications*, Lille, France, 1996.